



Comparison of Dielectric Properties between Epoxy Composites with Nanosized Clay Fillers Modified by Primary Amine and Tertiary Amine (Final draft (Post-print) version)

著者	Tagami Naoki, Hyuga Mayumi, Ohki Yoshimichi, Tanaka Toshikatsu, Imai Takahiro, Harada Miyuki, Ohchi Mitsukazu
journal or publication title	IEEE Transactions on Dielectrics and Electrical Insulation
volume	17
number	1
page range	214-220
year	2010
権利	IEEE Dielectrics and Electrical Insulation Society, The original publication is available at http://ieeexplore.ieee.org/stamp/stamp.jsp?tp=&arnumber=5412020
URL	http://hdl.handle.net/10112/5957

Comparison of Dielectric Properties between Epoxy Composites with
Nanosized Clay Fillers Modified by Primary Amine and Tertiary Amine
(Final draft (Post-print) version)

TAGAMI Naoki, HYUGA Mayumi, OHKI Yoshimichi, TANAKA Toshikatsu IMAI
Takahiro, HARADA Miyuki, OHCHI Mitsukazu

ABSTRACT

Epoxy-based nanocomposites (NCs) were prepared using clay modified by either primary amine or tertiary amine, and the effect of the difference in modifier on the thermal and dielectric properties of the NCs were discussed. The NC with clay fillers modified by the primary amine, 1C, shows a glass transition end temperature (T_{eg}) at a temperature 20 °C lower than the neat epoxy (N). This indicates that the resin of 1C is less crosslinked than that of N. On the other hand, the sample 3C, in which the clay was modified by the tertiary amine, shows a DSC spectrum close to that of N. Namely, 3C has a high crosslinking density similar to N. While the three samples show a relaxation peak in their dielectric loss spectra, the peak appears at high frequencies in 1C compared to N and 3C. Moreover, ionic conduction current flows more at high temperatures in 1C than in N or 3C. These facts are ascribable to the difference in their crosslinking densities.

Index Terms Epoxy nanocomposite, clay modifier, dielectric properties, DSC, electric conduction, complex permittivity.

1 INTRODUCTION

RECENTLY, various polymer nanocomposites (NCs), which are mixtures of base polymer and nanosized fillers, are attracting much attention as new materials with interesting properties in many fields including those of dielectrics and electrical

insulation^{1 2 3 4}. Especially, polymer/clay NCs in which nanosized clay fillers are dispersed into polymers such as epoxy resin⁵, polyamide⁶, and polypropylene⁷ are widely studied. A typical clay is montmorillonite consisting of stacked plate-like layers. Without any pre-modification, montmorillonite interlayers are hardly expanded and the clay fillers would not be well dispersed into a polymer. Therefore, modification to expand clay interlayers by use of swelling and cation exchanging reaction is important⁸. The mechanism through which the nanofiller loading yields superior dielectric properties has not been clarified yet, although it is generally assumed that the interaction between the polymer matrix and the filler should play a crucial role⁹. From this point of view, effects of clay modifiers on the surface property of the clay fillers and the resultant dielectric properties of NCs are examined in this paper by comparing primary amine and tertiary amine modifiers.

¹ T. Tanaka, "Dielectric nanocomposites with insulating properties", *IEEE Trans. Dielectr. Electr. Insul.*, Vol. 12, No. 5, pp. 914-928, 2005.

² M. F. Frechette, C. W. Reed, and H. Sedding, "Progress, understanding and challenges in the field of nanodielectrics", *IEEJ Trans. Fundamentals and Materials*, Vol. 126, No. 11, pp. 1031-1043, 2006.

³ T. Kikuma, N. Fuse, T. Tanaka, Y. Murata, and Y. Ohki, "Filler-content dependence of dielectric properties of low-density polyethylene/MgO nanocomposites", *IEEJ Trans. Fundamentals and Materials*, Vol. 126, No. 11, pp. 1072-1077, 2006.

⁴ J. C. Fothergill, J. K. Nelson, and M. Fu, "Dielectric properties of epoxy nanocomposites containing TiO₂, Al₂O₃ and ZnO fillers", 2004 Annual Report, Conf. Electr. Insul. Diele. Pheno., pp. 406-409, Boulder, 2004.

⁵ N. Tagami, M. Okada, N. Hirai, Y. Ohki, T. Tanaka, T. Imai, M. Harada, and M. Ochi, "Dielectric properties of epoxy/clay nanocomposites - Effect of curing agent and filler dispersion method-", *IEEE Trans. Dielectr. Electr. Insul.*, Vol. 15, No. 1, pp. 24-32, 2008.

⁶ N. Fuse, Y. Ohki, M. Kozako, and T. Tanaka, "Possible mechanisms of superior resistance of polyamide nanocomposites to partial discharges and plasmas", *IEEE Trans. Dielectr. Electr. Insul.*, Vol. 15, No. 1, pp. 161-169, 2008.

⁷ G. C. Montanari, D. Fabiani, F. Palmieri, D. Kaempfer, R. Thomann, and R. Mulhaupt, "Modification of electrical properties and performance of EVA and PP insulation through nanostructure by organophilic silicates", *IEEE Trans. Dielectr. Electr. Insul.*, Vol 11, No. 5, pp. 754- 762, 2004.

⁸ K. G. Gatos and J. Karger-Kocsis, "Effects of primary and quaternary amine intercalants on the organoclay dispersion in a sulfur-cured EPDM rubber", *Polymer*, Vol. 46, pp. 3069-3076, 2005.

⁹ T. Tanaka, M. Kozako, N. Fuse, and Y. Ohki, "Proposal of a multi-core model for polymer nanocomposite dielectrics", *IEEE Trans. Dielectr. Electr. Insul.*, Vol. 12, No. 4, pp. 669-681, 2008.

2 SAMPLES

The samples are neat epoxy resin, referred to as N in this paper, and two kinds of epoxy/clay NCs, namely 1C with clay fillers modified by primary amine and 3C with those modified by tertiary amine. The base epoxy resin is diglycidyl ether of bisphenol A cured with methylhexahydrophthalic anhydride, a kind of acid anhydride curing agent. The nanosized clay is a flake-like filler mainly composed of montmorillonite with an average width of 100 nm and a thickness of 1 nm. The clay content is 5 wt% constant for all the samples. There have been so many papers reporting that the best nanofiller content is somewhere around 1 to 7 wt% in many polymer nanocomposites [10] [11] [12] [13] [14] [15] [16]. We also examined the filler-content dependencies of various properties for the epoxy/clay nanocomposites before we started this research, and found that they showed good properties when the clay content was around 5 % [5] [16]. For the two NCs, in order to disperse clay fillers into the resin uniformly, a solubilization method was adopted, in which the clay fillers were modified by primary ocatadecylamine in 1C, and by tertiary dimethyldodecylamine in 3C. The

¹⁰ T. Kikuma, N. Fuse, T. Tanaka, Y. Murata, and Y. Ohki, "Filler-content dependence of dielectric properties of low-density polyethylene/MgO nanocomposites", *IEEJ Trans. Fundamentals and Materials*, Vol. 126, No. 11, pp. 1072-1077, 2006.

¹¹ N. Fuse, M. Kozako, T. Tanaka, S. Murase, and Y. Ohki, "Possible mechanism of superior partial-discharge resistance of polyamide nanocomposites", 2004 Annual Report, Conf. Electr. Insul. Diele. Pheno., pp. 322-325, Boulder, 2004.

¹² T. Kikuma, N. Fuse, T. Tanaka, Y. Murata, and Y. Ohki, "Dielectric properties of low-density polyethylene/MgO nanocomposites", 2006 Inter. Conf. Pro. Appli. Diele. Mater., pp. 323-326, 2006.

¹³ K. Ishimoto, T. Tanaka, Y. Ohki, Y. Sekiguchi, Y. Murata, and M. Gosyowaki, "Comparison of dielectric properties of low-density polyethylene/MgO composites with different size fillers", 2008 Annual Report, Conf. Electr. Insul. Diele. Pheno., pp. 208-211, Québec City, 2008.

¹⁴ M. Kozako, N. Fuse, Y. Ohki, T. Okamoto, and T. Tanaka, "Surface degradation of polyamide nanocomposites caused by partial discharges using IEC(b) electrodes", *IEEE Trans. Dielectr. Electr. Insul.*, Vol. 11, No. 5, pp.833-839, 2004.

¹⁵ Y. Ke, J. Lu, X. Yi, J. Zhao, and Z. Qi, "The Effects of Promoter and Curing Process on Exfoliation Behavior of Epoxy/Clay Nanocomposites", *J. Appl. Polym. Sci.*, Vol. 78, No. 4, pp. 808-815, 2000.

¹⁶ Y. Zhou, F. Pervin, V. K. Rangari, and Sh. Jeelani, "Influence of montmorillonite clay on the thermal and mechanical properties of conventional carbon fiber reinforced composites", *J. Mater. Process. Technol.*, Vol.191, No. 1-3, pp. 347-351, 2007

fillers were swollen in dimethylacetamide for both NCs [5]. These modifiers and solvents exfoliate the clay fillers, which brings about uniform dispersion of fillers. In addition, the tertiary amine also acts as a curing accelerator [17]. Figure 1 shows the chemical structures of the two modifiers. The clay fillers modified by the above method were dispersed in the epoxy resin by mixing them with a strong shear force to the sample in process. As shown in Figure 2, the clay fillers were exfoliated well and dispersed quite uniformly in both samples 1C and 3C.

3 EXPERIMENTAL METHODS

The sample's thermal properties were examined by differential scanning calorimetry (DSC) in a temperature range between 0 °C and 200 °C using Al₂O₃ as a reference. Furthermore, dc current was measured for 30 min by applying dc electric field of 5 kV/mm in a temperature range between 40 °C and 190 °C. The complex permittivity was measured with an impedance analyzer (Solartron 1296) in a frequency and temperature ranges from 10⁻¹ Hz to 10⁵ Hz and from 20 °C to 195 °C by applying ac voltage of 1 V_{rms} to 200- μ m-thick samples. For both dielectric permittivity and dc electric conductivity measurements, Au electrodes with a diameter of 20 mm ϕ were evaporated on each side of the sample. The two dielectric measurements were carried out in a chamber filled with N₂ at 1 atm in order to prevent color change due to oxidization of the resin, which is known to occur by heating epoxy resin in air at temperatures above 100 °C. For each experimental condition, measurements were repeated at least twice using different samples, and all the measurements showed good repeatability.

4 EXPERIMENTAL RESULTS

4.1 DSC

Figure 3 shows the DSC spectra. It is known that the glass transition temperature increases, keeping a good correlation with the crosslinking density¹⁷. Since the degree of crosslinking in epoxy resin is not uniform, glass transition occurs in a wide temperature range. Therefore, from the spectra, three glass transition temperatures, namely the initiation temperature (T_{ig}), the intermediate temperature (T_{mg}), and the end temperature (T_{eg}), are obtained and denoted by three different arrows in Figure 3

¹⁷ M. Ochi, K. Satake, Y. Nakanishi, N. Hata, and M. Tomoi [Ed.], *Sousetsu Epokishi-jushi Kisohen 1 (Epoxy Resins, Basics 1)*, The Japan Society of Epoxy Resin Technology: Tokyo, pp. 256-257 and 303, 2003 [in Japanese].

and by solid symbols (\blacktriangle , \bullet , \blacktriangledown) in Figure 4. The regions where the crosslinking density is high and low should be closely related to T_{eg} and T_{ig} , respectively. The three glass transition temperatures are clearly lower in 1C than in N, which would result from the fact that the epoxy matrix of 1C has a low crosslinking density¹⁸. On the other hand, 3C has similar T_{mg} and T_{eg} to N, although it has much lower T_{ig} . This fact indicates that the modification by tertiary amine can prevent the decrease in crosslinking density in the epoxy matrix caused by the nanoclay addition more effectively than the modification by primary amine.

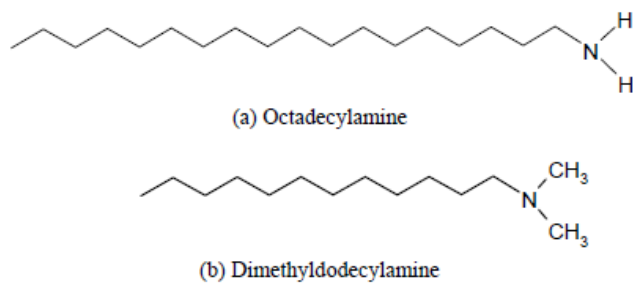


Figure 1. Chemical structures of the two clay modifiers. The primary octadecylamine was used for 1C, while the tertiary dimethyldodecylamine for 3C.

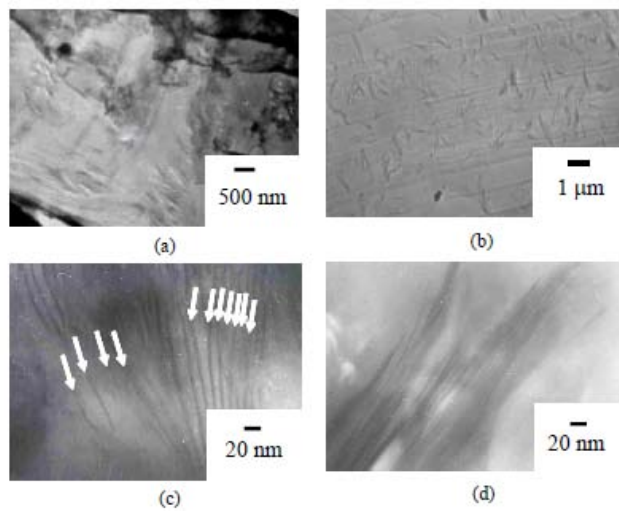


Figure 2. Transmission electron microscopy images of samples 1C (a, c) and 3C (b, d). The arrows in (c) indicate the clay fillers.

¹⁸ T. Liu, W. C. Tjiu, Y. Tong, C. He, S. S. Goh, and T. S. Chung, "Morphology and fracture behavior of intercalated epoxy/clay nanocomposites", J. Appl. Polym. Sci., Vol. 94, pp. 1236-1244, (200 4).

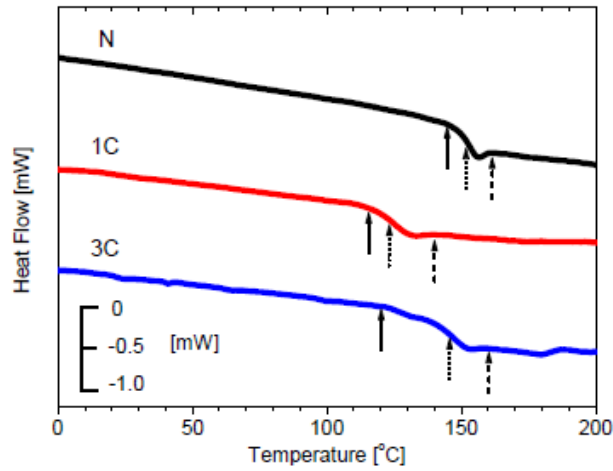


Figure 3. DSC spectra. The solid and dotted arrows show the glass transition initiation temperature (T_{ig}) and intermediate temperature (T_{mg}), while the dashed one shows its end temperature (T_{eg}).

4.2 ELECTRIC CONDUCTION

Nearly steady state current values observed 30 min after the start of voltage application are shown as a function of temperature in Figure 5. While the current is around 1 pA and is similar in all the samples at 40 °C, it is significantly higher in sample 1C than in the other two samples at 195 °C. The dotted line in Figure 5 shows 1 nA, and the temperature at which the current value becomes equal to 1 nA is referred to as TI1. Moreover, the temperature at which the current becomes 10 nA, which is shown by a dashed line in Figure 5, is referred to as TI2. Here, we chose the current values of 1 and 10 nA as indicators of two glass transition temperatures T_{ig} and T_{eg} , respectively, because the current values shown in Figure 5 are very close to 1 and 10 nA at T_{ig} and T_{eg} in all the samples. The two temperatures TI1 and TI2 thus measured are shown in Figure 4 with open symbols (\square , \circ). Both TI1 and TI2 are lower in 1C than in N. On the other hand, while TI1 for 3C is similar to that for 1C and is much lower than that for N, its TI2 is similar to that for N. This indicates that 3C has a superior insulation property at high temperatures. The temperature difference $TI2 - TI1$, which reflects the increment in current, is similar to that of the glass transition end point and its initial point $T_{eg} - T_{ig}$ for all the samples. From this fact, the electric conduction is governed significantly by the sample's thermal property.

4.3 COMPLEX PERMITTIVITY

Figure 6 shows the temperature dependencies of relative permittivity ϵ_r' and the

dielectric loss factor ϵ'' around the commercial frequency (56 Hz). Although there is a slight difference among the three samples, the values of ϵ' that are 3.6 in N, 3.6 in 1C, and 3.8 in 3C are almost the same within the experimental reproducibility at temperatures below 100 °C. There are also no differences in ϵ'' spectra among the three samples at temperatures below 100 °C. On the other hand, at temperatures above 100 °C, a significant difference is observed in 1C compared with the other two samples. Namely, while the temperature at which ϵ' and ϵ'' begin to show the rapid increase is 160 °C for N and 3C, it is 140 °C for 1C, which is 20 °C lower than N and 3C. Moreover, while ϵ' that shows an increase at 160 °C soon becomes saturated to 5.5 in N and to 6.0 in 3C, ϵ'' shows respective peaks at temperatures above 170 °C. In marked contrast to these two samples, in 1C, ϵ' and ϵ'' show a rapid monotonic increase with an increase in temperature, leading to a very high value at 195 °C.

Judging from the temperature dependencies of ϵ' and ϵ'' observed in samples N and 3C, the two samples have a relaxation process in a temperature range from 120 °C to 195 °C as shown in Figure 6. Therefore, ϵ' and ϵ'' are shown in Figure 7 as a function of frequency in this temperature region for three samples. In Figure 7a for N, while ϵ' is constantly 3.6 in the whole frequency range from 100 °C to 140 °C, a downward slope indicating the presence of a dielectric relaxation appears at temperatures above 170 °C. Corresponding to this ϵ' spectrum, a clear relaxation peak appears in Figure 7d at temperatures above 170 °C. Similar to N, 3C also exhibits similar relaxation at temperatures above 175 °C as shown in Figures 7c and f, although the presence of relaxation is not clear at 170 °C. Focusing on 1C, however, frequency dependencies of ϵ' and ϵ'' are quite different from those for N and 3C. Namely, ϵ' of 1C does not show a step that indicates the presence of relaxation at temperatures above

120 °C, while its ϵ' is constant at 3.5 in the whole frequency range at 100 °C similarly to the other two samples. Moreover, while ϵ'' of 1C exhibits a shoulder at temperatures above 170 °C in a frequency range between 103 and 5×10^4 Hz, no clear relaxation peaks appear as shown in Figure 7e.

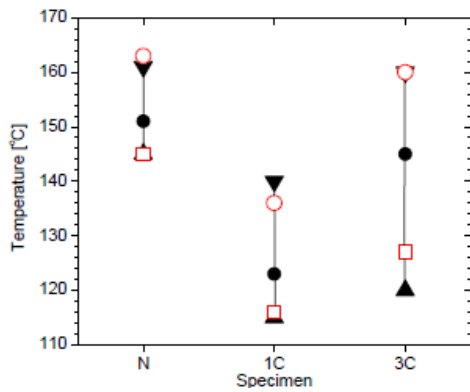


Figure 4. Comparison of T_{ig} , T_{mg} , T_{eg} , and the temperatures T_{I1} and T_{I2} at which the current becomes 1 nA and 10 nA, respectively. \blacktriangle : T_{ig} , \bullet : T_{mg} , \blacktriangledown : T_{eg} , \square : T_{I1} , \circ : T_{I2} .

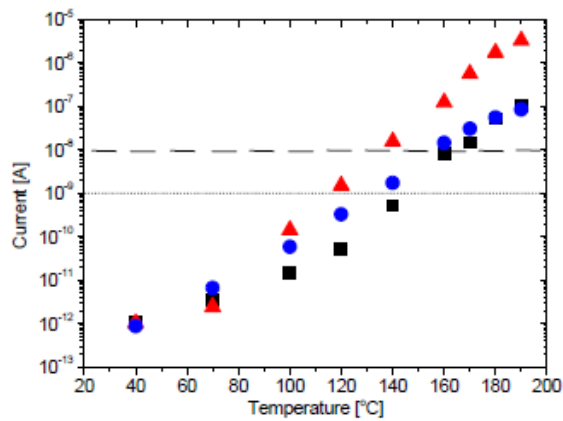
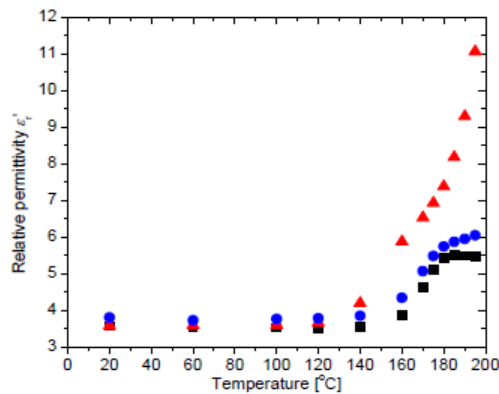
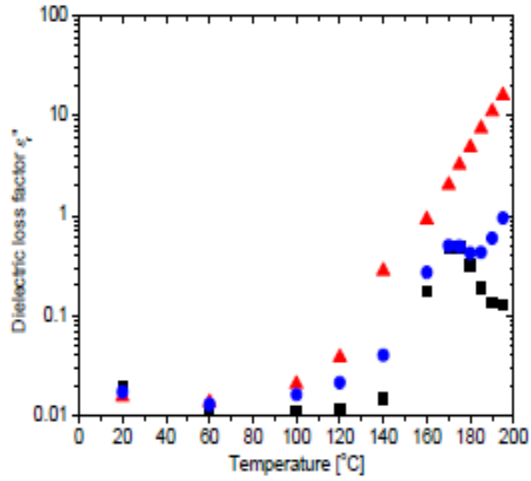


Figure 5. Values of current observed 30 min after the application of dc 5 kV/mm. The dotted line shows 1 nA, while the dashed line shows 10 nA. \blacksquare : N, \blacktriangle : 1C, \bullet : 3C.



(a) Dielectric constant



(b) Dielectric loss factor

Figure 6. Temperature dependencies of relative permittivity and dielectric loss factor around the commercial frequency (56 Hz). ■ : N, ▲ : 1C, ● : 3C.

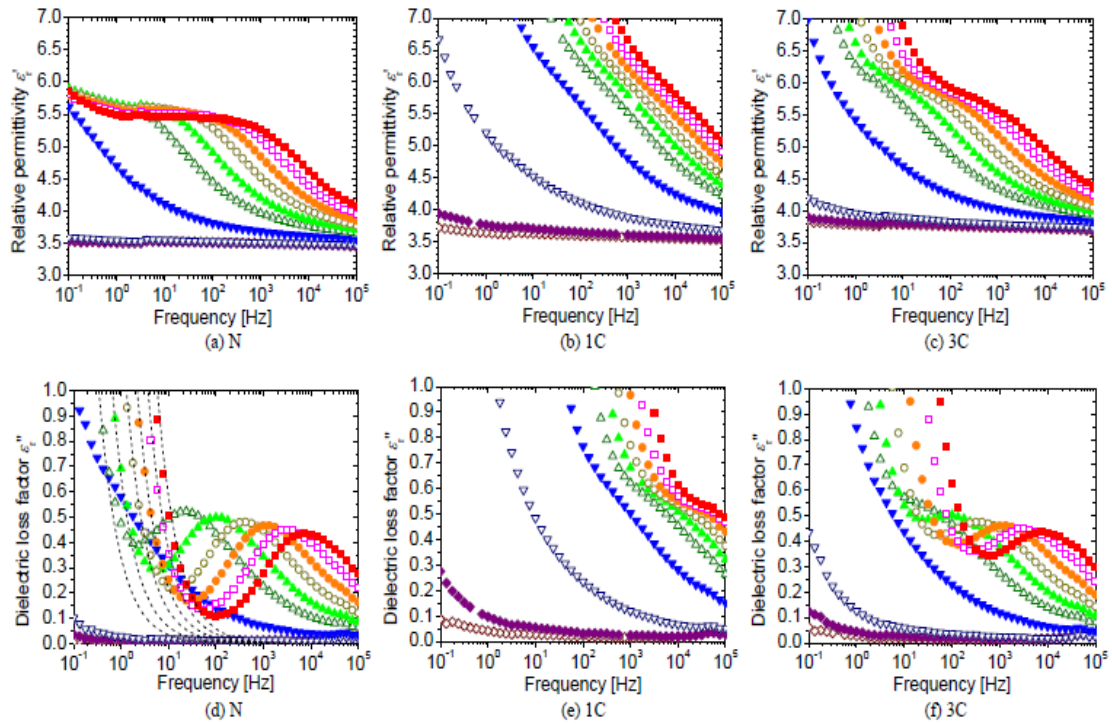


Figure 7. Change in the complex permittivity as a function of temperature. ◇ : 100 °C, ◆ : 120 °C, ▽ : 140 °C, ▾ : 160 °C, △ : 170 °C, ▲ : 175 °C, ○ : 180 °C, ● : 185 °C, □ : 190 °C, ■ : 195 °C.

5 DISCUSSION

In Figure 4, the temperature difference $T_{I2} - T_{I1}$, which is an indicator of the sharpness of current increase is quite similar to that of $T_{eg} - T_{ig}$. This fact indicates that the current increase is actually governed by the glass transition in all the samples. In other words, the current in the bulk is controlled by the molecular motion in the epoxy matrix. Namely, in the epoxy/clay NCs, nanoclay plays a role as a dynamical factor to restrict or activate the molecular motion of the epoxy resin¹⁹ rather than it acts as a charge trap or a hopping-site²⁰. From this viewpoint, the molecular motion of the epoxy matrix is evaluated by analyzing the above-mentioned relaxation process seen in the complex permittivity spectra and its relation to the electric conduction in the samples. The rapid increase in ϵ_r' and ϵ_r'' seen in the low frequency region in Figure 7 is caused by the electric conduction. Provided that the dc electric conduction ascribable to conductivity σ is effective, ϵ_r'' should be contributed by σ as described by the equation,

$$\epsilon_r'' = \frac{\sigma}{2\pi\epsilon_0 f}, \quad (1)$$

where ϵ_0 is the permittivity of vacuum and f is the frequency of the applied voltage²¹. Because σ is very high, especially in 1C, at high temperatures as shown in Figure 5, the conductivity component appears in ϵ_r'' obviously in Figure 7e. Moreover, when charge exchange does not occur on the electrodes, heterocharge accumulates in the vicinity of their surfaces. This results in the increase in charge density on the electrodes, which in turn increases ϵ_r' . The rapidly increased portions in the ϵ_r'' spectra can be fitted very well by Eq. (1) as typically shown by dashed curves in Figure 7d. By drawing such a fitting curve to each ϵ_r'' spectrum, the conductivity component was subtracted in order to obtain the ϵ_r'' component due to the relaxation. Figure 8 shows the obtained relaxation component spectra, in which clear Debye type dielectric relaxation peaks are seen. For example, the peak appears at 24, 2.4×10^3 , and 42 Hz for

¹⁹ N. Fuse, Y. Ohki, M. Kozako, and T. Tanaka, "Possible mechanisms of superior resistance of polyamide nanocomposites to partial discharges and plasmas", *IEEE Trans. Dielectr. Electr. Insul.*, Vol. 15, No. 1, pp. 161-169, 2008.

²⁰ Y. Murata, Y. Sekiguchi, Y. Inoue, and M. Kanaoka, "Investigation of electrical phenomena of inorganic-filler/LDPE nanocomposite material", *Proc. of Inter. Symp. Electr. Insul. Mater.*, Vol. 3, pp. 650-653, Kitakyushu, 2005.

²¹ N. Tagami, M. Okada, N. Hirai, Y. Ohki, T. Tanaka, T. Imai, M. Harada, and M. Ochi, "Dielectric properties of epoxy/clay nanocomposites - Effect of curing agent and filler dispersion method-", *IEEE Trans. Dielectr. Electr. Insul.*, Vol. 15, No. 1, pp. 24-32, 2008.

N, 1C, and 3C, respectively, at 170 °C. Assuming that the relaxation seen in Figures 7d to f and Figure 8 is of a single Debye type, the relaxation time τ satisfies the equation,

$$\tau = \frac{1}{2\pi f_m}, \quad (2)$$

where f_m is the frequency at which ϵ'' becomes the maximum. At temperatures above 170 °C, τ is shorter in 1C and similar in N and 3C. The calculated values of τ are shown in Figure 9. Figure 9 also shows the electric resistivity ρ calculated from the conduction current shown in Figure 5 at temperatures between 160 °C and 190 °C. It can be seen that τ and ρ are similar in both the sample and temperature dependencies. Namely, the difficulty in molecular motion denoted by τ and the difficulty in electric conduction denoted by ρ are positively correlated. Here, σ , which is the reciprocal of ρ , is expressed as a product of the free charge density ρ_c and its mobility μ . Since ionic conduction is dominant in the electric conduction in epoxy resin similarly to other many polymers²², Figure 9 indicates that the ion mobility μ in the epoxy resin positively correlates to the easiness of molecular motion in the epoxy matrix. Considering the discussion developed above, in the case of the sample 1C, the molecular motion in the epoxy matrix is easy, which results in high ion mobility. On the other hand, the molecular motion is not activated by the nanoclay addition in the case of 3C. Therefore, the degree of molecular motion and the ion mobility in 3C are similar to those of N. This difference is due to the difference in the effects of clay modifiers on the polymer networks. The filler addition inherently hinders the formation of polymer networks and crosslinks. In the case of 3C, the modifier, tertiary dimethyldodecylamine, can act as a curing accelerator as mentioned above²³. Therefore, the degree of molecular motion remains similar to N. However, in the case of 1C, the crosslinking density decreases by the addition of fillers.

6 CONCLUSION

Effects of the modifier on the thermal and dielectric properties of epoxy-based nanocomposites (NCs) were investigated using neat epoxy resin and its NCs with nanosized clay fillers modified by either primary amine or tertiary amine.

²² M. Shimbo [Ed.], *Epokishi-jushi Handobukku (Epoxy Resin Handbook)*, Nikkan Kogyo Shinbun: Tokyo, p. 338, 1987 [in Japanese].

²³ M. Ochi, K. Satake, Y. Nakanishi, N. Hata, and M. Tomoi [Ed.], *Sousetsu Epokishi-jushi Kisohen I (Epoxy Resins, Basics I)*, The Japan Society of Epoxy Resin Technology: Tokyo, pp. 256-257 and 303, 2003 [in Japanese].

1. The glass transition end temperature (T_g) of NC with clay fillers modified by the primary amine (1C) is 140 °C, which is 20 °C lower than that of the neat epoxy resin (N), 161 °C. On the other hand, NC with clay fillers modified by the tertiary amine (3C) shows T_g similar to N. Therefore, the clay modification by the tertiary amine would prevent the decrease in crosslinking density of the resin.

2. At 180 °C, which is above T_g , the resistivity of 1C is about 1/30 of that of N, while 3C has a high resistivity similar to N. This indicates that the modification by the tertiary amine provides good insulating properties to the epoxy/clay NC.

3. While the relaxation time due to the dipolar relaxation, appearing in 1C at high temperatures above T_g , is about 1/20 of that in N, 3C shows a long relaxation time similar to N.

4. Since the above-mentioned relaxation time of each sample positively correlates to its resistivity, the nanoclay would exert a certain effect on the ion mobility that is assisted by the molecular motion in the epoxy resin.

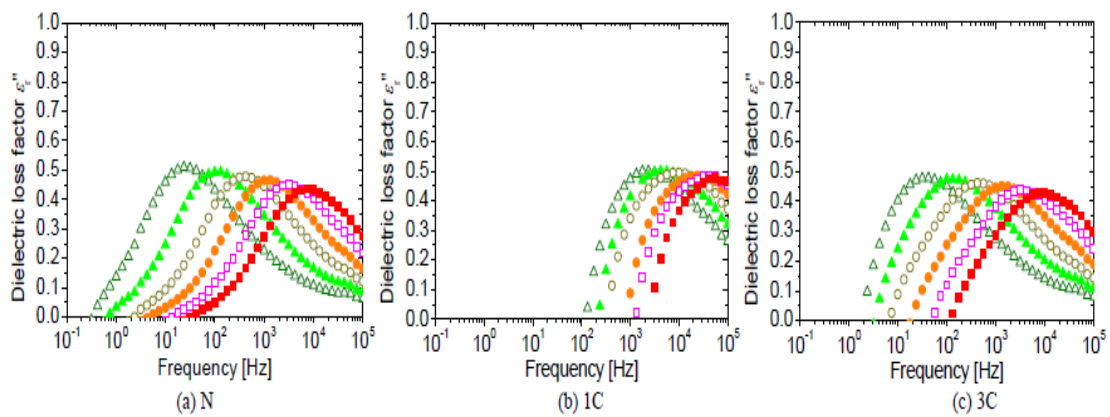


Figure 8. Frequency dependencies of ϵ'' , from which the contribution of dc conduction was removed, in a temperature range between 170 °C and 195 °C. Δ : 170 °C, \blacktriangle : 175 °C, \circ : 180 °C, \bullet : 185 °C, \square : 190 °C, \blacksquare : 195 °C. 2.10 2.15

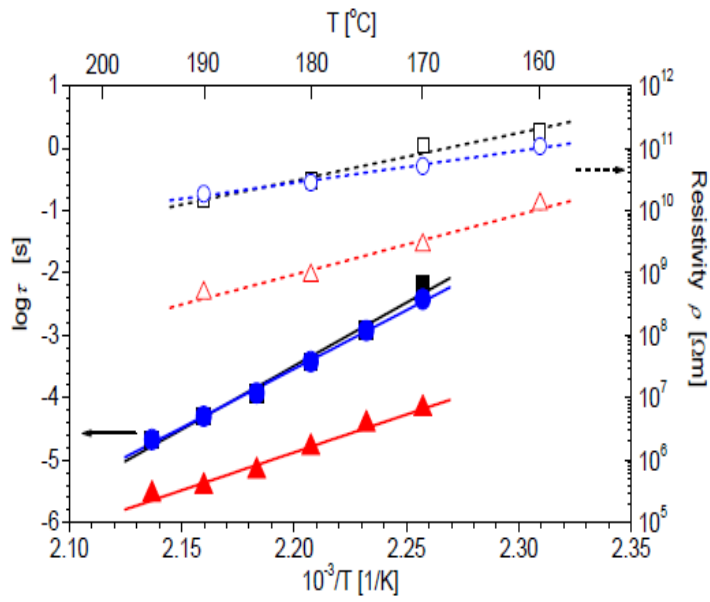


Figure 9. Reciprocal temperature dependencies of relaxation time (τ) and resistivity (ρ). The solid symbols with solid lines and the open symbols with dotted lines show τ and ρ , respectively. Here, τ is shown at intervals of 5 °C from 170 °C to 195 °C, and ρ is shown at intervals of 10 °C from 160 °C to 190 °C. ■, □: N, ▲, △: 1C, ●, ○: 3C.